© 2019. Published by The Company of Biologists Ltd | Development (2019) 146, dev175976. doi:10.1242/dev.175976

RESEARCH REPORT

The development of CRISPR for a mollusc establishes the formin *Lsdia1* as the long-sought gene for snail dextral/sinistral coiling

Masanori Abe[1,*] and Reiko Kuroda[1,2,*,‡]

ABSTRACT

The establishment of left-right body asymmetry is a key biological process that is tightly regulated genetically. In the first application of CRISPR/Cas9 to a mollusc, we show decisively that the actin-related diaphanous gene *Lsdia1* is the single maternal gene that determines the shell coiling direction of the freshwater snail *Lymnaea stagnalis*. Biallelic frameshift mutations of the gene produced sinistrally coiled offspring generation after generation, in the otherwise totally dextral genetic background. This is the gene sought for over a century. We also show that the gene sets the chirality at the one-cell stage, the earliest observed symmetry-breaking event linked directly to body handedness in the animal kingdom. The early intracellular chirality is superseded by the inter-cellular chirality during the 3rd cleavage, leading to asymmetric *nodal* and *Pitx* expression, and then to organismal body handedness. Thus, our findings have important implications for chiromorphogenesis in invertebrates as well as vertebrates, including humans, and for the evolution of snail chirality.

This article has an associated 'The people behind the papers' interview.

KEY WORDS: Left-right, Handedness, Asymmetry, Chirality, CRISPR/Cas9, Formin

INTRODUCTION

Left-right body asymmetry is established by tightly regulated genetic processes. Interest has centred on the diverse mechanisms proposed for different phyla, the possibility of a unified mechanism (Blum et al., 2014; Coutelis et al., 2014; Juan et al., 2018; Nakamura and Hamada, 2012; Tingler et al., 2018; Vandenberg and Levin, 2013) and the involvement of cellular chirality (Danilchik et al., 2006; González-Morales et al., 2015; Meshcheryakov and Beloussov, 1975; Schonegg et al., 2014; Taniguchi et al., 2011; Tee et al., 2016; Wan et al., 2011); however, many important aspects are unresolved. To study the molecular and cellular mechanisms of chiromorphogenesis, we have used the snail *Lymnaea* (*L.*) *stagnalis* as an organism with unique advantages. Notably, it has both the sinistral (recessive) and the dextral (dominant) strains within a species; it is a hermaphrodite that both self- and cross-fertilizes; and the chirality of the related *L. peregra* (Boycott and Diver, 1923; Freeman and Lundelius, 1982; Sturtevant, 1923) and of *L. stagnalis* (Asami et al., 2008; Hosoiri et al., 2003; Kuroda et al., 2009; Shibazaki et al., 2004) species has been suggested but not proven to be determined by a single locus that functions maternally. We have recently identified the actin-related diaphanous gene *Lsdia1* as a candidate for the handedness-determining gene by positional cloning (Kuroda, 2014; Kuroda et al., 2016). *Lsdia1* (3261 bp and 1087 amino acids) is expressed maternally and the protein is present from ovipositioning to the gastrulation stage in the dextral strains. By contrast, in the sinistral strains, both of the *Lsdia1* alleles carry a frameshift mutation early in the coding region (c.184delC) that leads to protein truncation (p.Leu62Serfs*24) (Kuroda et al., 2016) (Fig. 1A). The loss of LsDia1 in the sinistral strains is compensated for by the presence of the tandemly duplicated *Lsdia2* gene, the protein product of which has 89.4% amino acid similarity to LsDia1 (Kuroda et al., 2016). *Lsdia2* (3297 bp, 1099 amino acids) is also expressed maternally at the one-cell stage in both dextral and sinistral snails (Kuroda et al., 2016).

Another group (Davison et al., 2016) has also reported that Dia is associated with left-right asymmetry; however, their key results do not agree with ours. Notably, the whole-mount *in situ* hybridization results are opposite for the two studies. We observed no localization of *Lsdia1* mRNA (Kuroda et al., 2016), in contrast to Davison's strong asymmetrically localized expression of *dia* as well as *fry* mRNAs confined to one of the blastomeres or to part of a blastomere in the two- and four-cell-stage embryos. Second, we could selectively target *Lsdia1* mRNA based on our sequencing of *Lsdia1* and *Lsdia2* genes; however, they could not discriminate the two mRNAs in their whole-mount *in situ* hybridization experiments because of DNA sequence differences from ours in some parts. Finally, regarding the formin inhibition experiments used for corroboration, owing to lethality even at 5.0 µM inhibitor concentration, we concluded that these experiments do not provide any meaningful insights (Kuroda et al., 2016). Davison et al., on the other hand, drew a conclusion based on their results with 100 µM inhibitor concentration. Regardless of these key differences, the 2016 papers left open the likely possibility that the key mutation was genetically linked to the mutation we found, rather than being the mutation we found itself. Thus, although the 2016 papers attempted to identify the key gene, decisive identification has awaited the construction and testing of independent mutants with the same effects. Accordingly, we aimed to identify the gene by directly knocking out *Lsdia1* using CRISPR/Cas9.

RESULTS AND DISCUSSION

CRISPR/Cas9 knockouts invert snail shell coiling

To establish that *Lsdia1* is the handedness-determining gene and to elucidate what role *Lsdia1* has in the cellular programme that directs snail chirality, we developed *Lsdia1*-targeted CRISPR/Cas9

[1]Research Institute for Science and Technology, Tokyo University of Science, 2641 Yamazaki, Noda-shi, Chiba, 278-8510, Japan. [2]Department of Applied Biological Science, Graduate School of Science and Technology, Tokyo University of Science, 2641 Yamazaki, Noda-shi, Chiba, 278-8510, Japan.

*Present address: Institute of Science and Technology Research, Chubu University, 1200 Matsumoto-cho, Kasugai, Aichi, 487-8501 Japan.

‡Author for correspondence (rkuroda@isc.chubu.ac.jp)

M.A., 0000-0003-4016-9583; R.K., 0000-0002-0268-7729

Received 20 January 2019; Accepted 11 April 2019

Development (2019) 146, dev175976. doi:10.1242/dev.175976

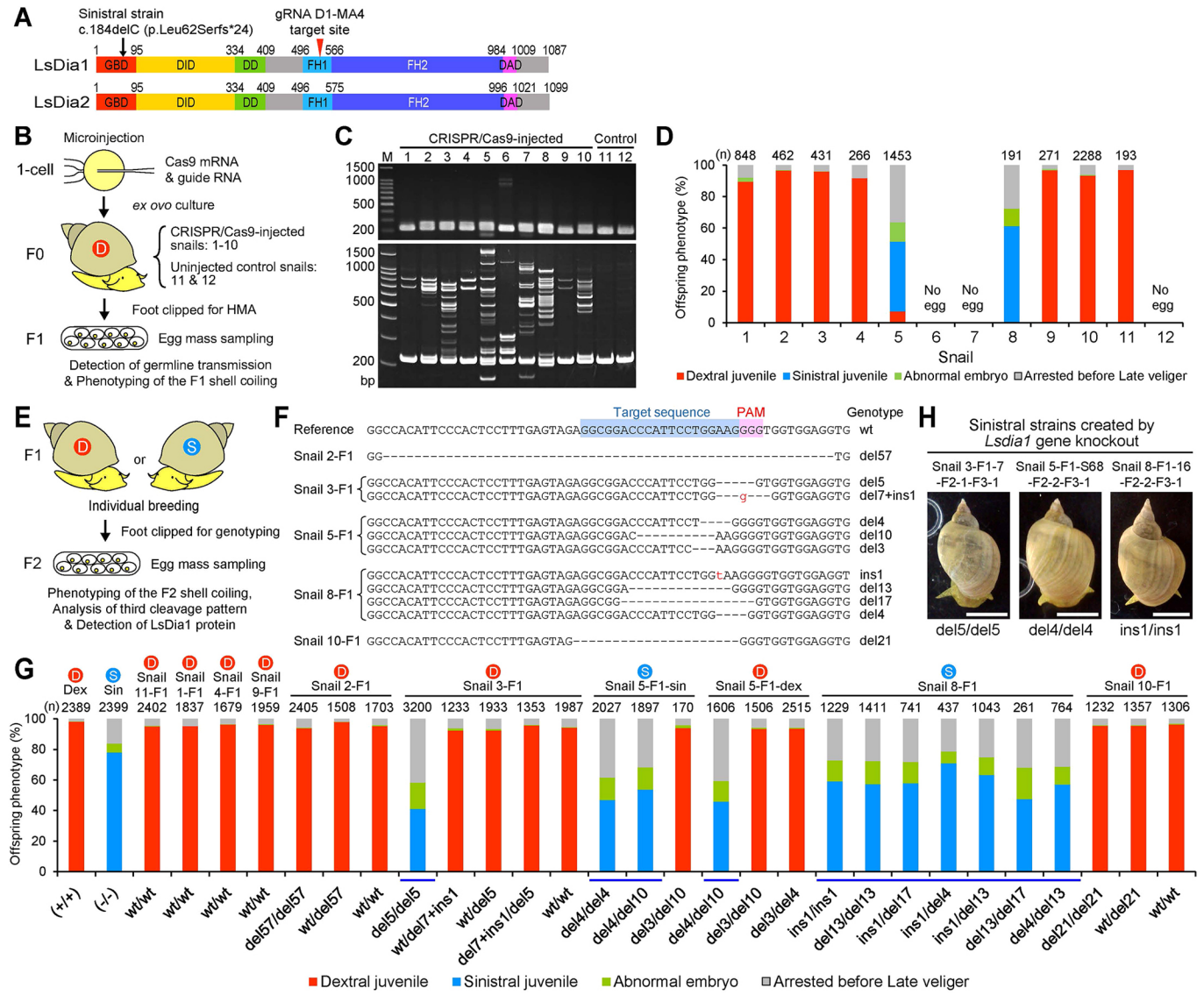

Fig. 1. Inactivation of *Lsdia1* by CRISPR/Cas9 reverses snail shell coiling. (A) Structures of LsDia1 and LsDia2. GBD, Rho GTPase-binding domain; DID, diaphanous inhibitory domain; DD, dimerization domain; FH1 and FH2, formin homology domains 1 and 2; DAD, diaphanous autoregulatory domain. Protospacer adjacent motif (PAM) and target sequences were designed in the FH1 region of *Lsdia1* (red arrowhead) to discriminate *Lsdia1* from *Lsdia2* (Fig. S1A). (B) Flow of experiments: Cas9 mRNA and guide RNA were injected into the dextral snail eggs at the one-cell stage, and these embryos were carefully raised to adult F0 snails. HMA was performed on DNA from the clipped foot of ten CRISPR/Cas9-injected (1-10) and two control (11-12) adult snails (Fig. S1B). Adult snails were self-fertilized to produce the F1 generation. Five to ten eggs from each egg mass were directly subjected to PCR amplification and HMA (Fig. S2A), and the rest of the embryos were reared to F1 juveniles to check their chirality. (C) HMA of the F0 generation by 2% agarose gel (top) and 10% polyacrylamide gel (bottom) electrophoresis. (D) Bar chart of shell coiling of the F1 generation. No offspring were produced from snails 6, 7 and 12. The total number of embryos studied (*n*) is shown on the top of the bar graph. (E) Flow of experiments: F1 were individually bred and their genotype was determined from clipped foot DNA. (F) Comparison of the target sequence for the germline transmitted F1 (snails 2, 3, 5, 8 and 10). (G) Bar chart of offspring (F2) phenotype examined at the juvenile stage for each F1 genotype (bottom of the bar chart), including wild-type Dex (+/+), Sin (–/–), control (snail 11) and non-edited F1 (snails 1, 4, 9). The total number of embryos studied (*n*) is shown on the top of the bar graph. Homozygous knockout mutants (blue line, $P<0.0001$). D in a red circle and S in a blue circle indicate dextral and sinistral snails, respectively. Eggs produced by self-fertilization of F1 were used to check the presence of LsDia1 protein in the one-cell embryos (Fig. 2D), the cleavage pattern/cytoskeletal dynamics at the 3rd cleavage (Fig. 2A-C) and the F2 phenotype (G). (H) Photographs of healthy sinistral strains (F3) created by the *Lsdia1* gene knockouts. Scale bars: 1 cm.

techniques (Jinek et al., 2012) to create gene-knockout snails (Fig. 1A,B). Out of four independent injection experiments, we obtained 10 CRISPR/Cas9-injected adult snails (numbered 1-10) and two control adult snails (11-12) (Fig. S1B,C). By using DNA extracted from the clipped foot while keeping the snails alive, heteroduplex mobility assays (HMA) (Zhu et al., 2014) were carried out on the snails (Fig. 1B), which showed mosaic mutational patterns at the F0 stage (Fig. 1C). Germline transmission to F1 embryos occurred in snails 2, 3, 5, 8 and 10, of which snails 2, 3 and 10 produced only dextral offspring, whereas snail 8 had only sinistral offspring (Fig. 1D; Fig. S2; Table S1). Remarkably, snail 5 produced both dextral and sinistral F1 (denoted as 5-F1-dex and 5-F1-sin) within an egg mass (Fig. S2B; Table S1). This must be a consequence of mosaicity of frameshift and non-frameshift mutations introduced into the tissues of the gonad at F0, which are originated from the 4d mesentoblast (Morrill, 1998). When and where in the gonad the *Lsdia1* mRNA is transcribed and provided to the oocyte is an interesting unresolved issue.

Development (2019) 146, dev175976. doi:10.1242/dev.175976

To prove the shell coiling direction is really the maternal effect of the edited *Lsdia1* gene, we studied the F2 generation where the genotype is homogeneous throughout the body (Fig. 1E). PCR genotyping of F1 adult snails showed only a limited number of mutation patterns in each F0 (Fig. 1F; Table S2). By analysis of many thousands of offspring from each F1 lineage, it is clear that F1 snails with a homozygous knockout mutation (e.g. del5/del5, del13/del17) produced sinistral snails. By contrast, snails with biallelic non-frameshift mutations (e.g. del57/del57) or with heterozygous knockouts where at least one of the alleles possesses no mutation (wt) or a non-frameshift mutation (e.g. wt/del5, del3/del10) produced only the dextral F2 generation (Fig. 1G). This outcome was also observed for 5-F1-dex and 5-F1-sin, regardless of the body handedness of the mother (Fig. 1G; details in Table S2). Clearly, the genetic chirality control introduced by the CRISPR/Cas9 at F0 is stably inherited and continues generation after generation (verified up to F4) (F3 in Fig. 1H; Fig. S3; Tables S1, S2). This is in sharp contrast to the mechanically induced mirror-image snails whose effect lasts one generation only (Kuroda et al., 2009). Sinistral-specific species such as *Physa acuta* and *Indoplanorbis exustus* carry only the *dia* type 2 gene (Kuroda et al., 2016). Thus, our gene-editing results are interesting as they may eventually lead to the generation of a new species (Hoso et al., 2010). We have confirmed that there was no gene editing in *Lsdia2*. Moreover, off-target effects are unlikely as clear and consistent results were obtained from independent CRISPR/Cas9 experiments.

Third-cleavage patterns are dictated by *Lsdia1*: the handedness-determining gene

Cytoskeletal dynamics at the crucial 3rd cleavage (four- to eight-cell stage) is also controlled by the *Lsdia1* genotype. This stage displays the first definitive chirality, i.e. clockwise (CW) and anti-clockwise (ACW) micromere rotation for the dextral and the sinistral embryos, respectively, and the CW micromere rotation of dextral embryos is accompanied by the spiral deformation of macromeres (SD) and the consequent spindle inclination (SI). In the sinistral embryos, spindles are radially positioned (no SI) and micromeres are formed just above the macromeres without SD, which are then rotated levotropically (Shibazaki et al., 2004; Kuroda, 2014, 2015; Kuroda et al., 2009, 2016). We have checked the 3rd-cleavage pattern of progeny of F1 and classified it in the same way as we previously classified the wild-type embryos (Kuroda, 2014). Progeny of F1 with biallelic non-frameshift mutants and heterozygous knockouts exhibited CW rotation with SD and SI, just like the wild-type dextral strains, even with up to a 57-base pair deletion in both alleles (Fig. 2A-C; Fig. S4). By contrast, offspring of F1 snails with homozygous knockouts exhibited varied cleavage patterns similar to the wild-type (−/−) sinistral embryos, i.e. mostly ACW, but sometimes partial ACW, neutral and very rarely partial CW and CW, with no SD/SI in all these cases (Fig. 2A-C; Fig. S4; Movies 1-3). SD ensures correct direction and sufficient degree of micromere rotation at the 3rd cleavage. Hence, homozygous knockout or wild-type (−/−) sinistral embryos without this control sometimes result in micromere rotations other than ACW, leading to abnormal development (Kuroda, 2014) (Fig. 1G; Tables S1, S2). The marginally higher incidence of the unusual development in the offspring of homozygous knockout mothers may be due to the fact that CRISPR/Cas9-mediated homozygous knockout allows the translation of the protein up to the FH1 domain (Fig. 1A) and thus, the partial proteins may interfere with the activities of LsDia2 protein. The interpretation that the very rare dextrality that emerged is not associated with genetic changes is supported by the finding that sinistral F3 offspring were born from the dextral snails according to the F2 genotype (Fig. S5; Table S2).

Presence of LsDia1 protein at the one-cell stage depends on the maternal genotype

Evidence for *Lsdia1* as the handedness-determining gene is further strengthened by western blot analyses carried out for each F1 genotype. A perfect correlation was found between the presence and absence of the protein in the one-cell embryos immediately after ovipositioning and the maternal genotype (Fig. 2D). It appears that

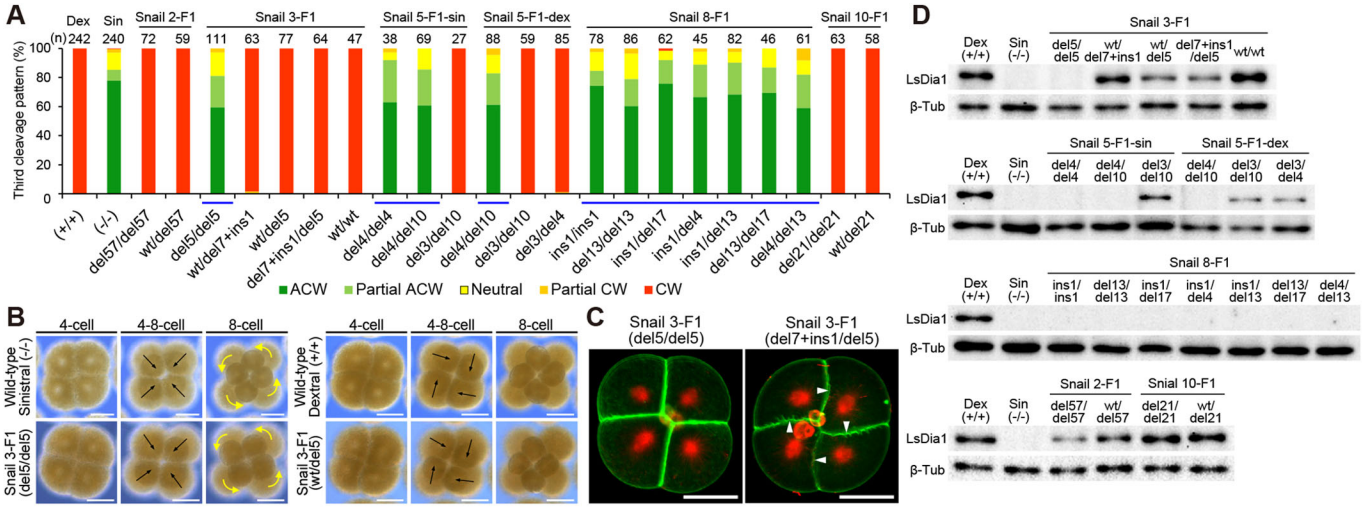

Fig. 2. Genotype of the gene-edited mother determines the cytoskeletal dynamics at the 3rd cleavage and the presence/absence of LsDia1 protein at the one-cell stage of her offspring. (A) Bar chart of the 3rd cleavage patterns of progeny of F1 for each genotype, together with that of wild type (+/+) and (−/−). The pattern was classified as previously reported (Kuroda, 2014); ACW, partial ACW, neutral, partial CW and CW. The total number of embryos studied (*n*) is shown on the top of each bar. Homozygous knockout mutants (blue line, $P<0.0001$). (B) Time-lapse images of the 3rd cleavage patterning. Black arrows indicate the direction of spindles; yellow curved arrows show the direction of micromere rotation. Scale bars: 50 µm. (C) Embryos of snails 3-F1 (del5/del5) and 3-F1 (del7+ins1/del5) at the metaphase-anaphase stage of the 3rd cleavage. Double staining for filamentous actin was carried out using Alexa Fluor 488-labelled phalloidin (green) and β-tubulin was visualized using Cy3-labelled anti-β-tubulin antibody (red). White arrowheads indicate the direction of SD for the dextral embryos. Scale bars: 50 µm. (D) Western blot analyses at the one-cell stage of F2 embryos for each representative genotype of F1. The target site of the anti-LsDia1 antibody is at the C-terminal region (Kuroda et al., 2016).

Development (2019) 146, dev175976. doi:10.1242/dev.175976

LsDia1 protein present in oviposited embryos induces dextral spiral cleavage with SD and SI. Involvement of the actin cytoskeleton during the 3rd cleavage is in agreement with our previous finding that agents inhibiting actin but not microtubule polymerization destroyed SD (Shibazaki et al., 2004).

Snail chirality is initially determined from the one-cell stage by *Lsdia1*

Body handedness of *L. stagnalis* is uniquely established at the 3rd cleavage (Kuroda et al., 2009). Is this the first observable chirality? When is chirality first exhibited in development? To address this important issue, we used trypsin treatment of the one-cell-stage embryos to decrease the vitelline membrane tension, a method first described by Meshcheryakov and Beloussov (1975). We revealed, for the first time, substantial mirror-image chirality for the sinistral and dextral embryos within a species at the 1st cleavage. Remarkably, the chirality depended on the maternal *Lsdia1* genotype regardless of whether it is for the wild-type or the gene-edited embryos (Fig. 3A,B; Movie 4). The observations indicate that the single fertilized egg carries intrinsic left or right chirality information depending on the absence or presence of functional LsDia1 protein. This is the earliest observed symmetry-breaking event linked directly to body handedness in the phyla of the animal kingdom (Blum et al., 2014; Coutelis et al., 2014; Schonegg et al., 2014; Vandenberg and Levin, 2013).

The mirror-relationship of cytoskeletal dynamics between the dextral and sinistral embryos within a species is kept until the end of the 2nd cleavage but broken at the crucial 3rd cleavage where only the dominant dextral embryos exhibit SD/SI (Shibazaki et al., 2004; Kuroda et al., 2009). It seems that chirality is realized initially using the information contained within each blastomere. This may solve the enigma whereby micromeres of sinistral embryos rotate only ACW at the 3rd cleavage after the non-chiral emergence from the macromeres, rather than equally both ACW and CW. During and after the 3rd cleavage, cell-cell interactions become dominant, which can overwrite the initial intracellular chirality if appropriately forced by artificial external power, and establish definitive chirality.

Sites of *nodal* and *Pitx* gene expression are reversed for *Lsdia1* knockouts, resulting in mirror-imaged animals

Chiromorphogenesis at the organismal level is achieved by asymmetric expression of *nodal* and *Pitx* genes in both invertebrates and vertebrates (Abe et al., 2014; Blum et al., 2014; Coutelis et al., 2014; Grande and Patel, 2009; Kuroda, 2014; Kuroda et al., 2009; Vandenberg and Levin, 2013). We have previously shown that *nodal* and *Pitx* gene expression in *L. stagnalis* starts at the early cell stages of 33-49 and 49-64, respectively, and continues up to veliger stage (Kuroda, 2015), following the chirality of the eight-cell blastomere arrangement even when that is reversed by mechanical manipulation (Kuroda, 2014). We could show (Fig. 4) that homozygous knockout embryos produced by the gene-edited F1 snails exhibited *nodal* and *Pitx* gene expression patterns that were complete mirror images of the original dextral embryos, whereas expression in heterozygous knockout snails was just like the wild-type dextral embryos (Kuroda, 2015; Kuroda et al., 2009). Thus, *nodal* and *Pitx* expression patterns are also determined by the presence of LsDia1 protein.

How is the chirality that is established at the 3rd cleavage transmitted to produce asymmetric *nodal* and *Pitx* expression? We identified the cell that first expresses the *nodal* gene as cell $2c^{12}$ at the 49-cell stage and that of *Pitx* as $2d^{212}$ at the 64-cell stage. Thus, the 24-cell stage at which the cell fates are determined

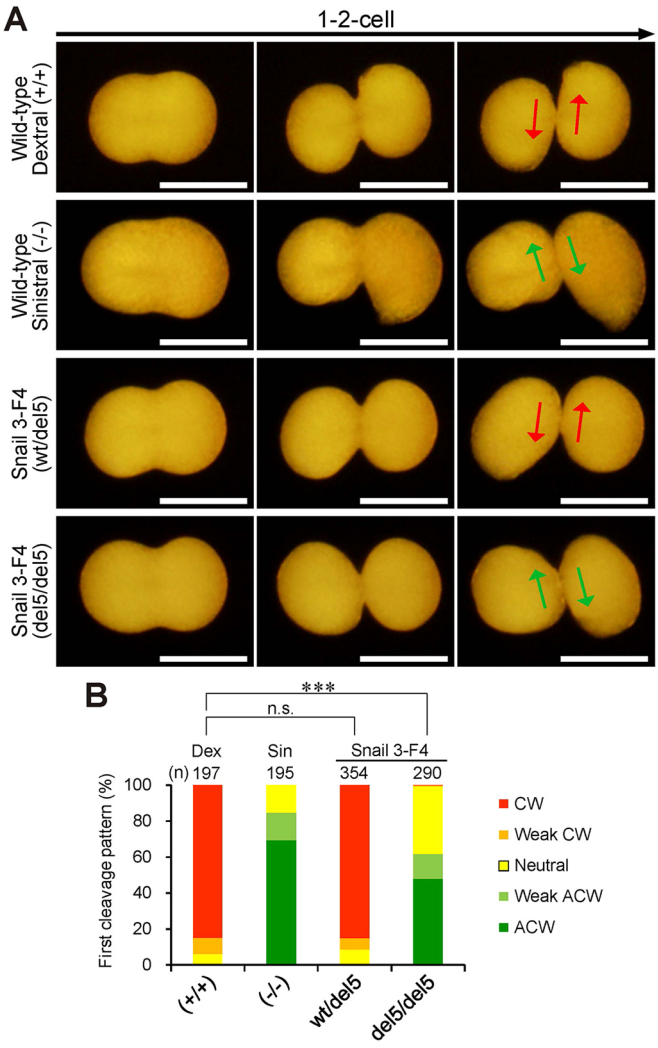

Fig. 3. *Lsdia1* genotype-linked mirror-image chirality at the 1st cleavage for the sinistral and dextral embryos. (A) Time-lapse images (animal view) of the 1st cleavage of the embryos treated with trypsin (see text) for the wild-type (*Lsdia1*+/*Lsdia1*+) (–/–) and gene-edited 3-F4 (del5/del5 and wt/del5). Arrows indicate the twisting direction of the blastomeres: CW (red) and ACW (green). Scale bars: 100 µm. (B) Bar chart of the twisting patterns observed in A, classified as CW, weak CW, neutral, weak ACW and ACW. *n* is the total number of embryos studied in the four egg masses of each genotype. ***P<0.0001; n.s., non-significant.

(Martindale, 1986) must be a crucial period in the transfer of chiral information.

In this study, using the first successful gene knockouts in Mollusca, we revealed novel mechanistic features of left-right asymmetry establishment in *L. stagnalis* and its dependence on the actin-related LsDia1 protein. First, we present decisive genetic evidence that expression of *Lsdia1* determines the outcome of left-right body asymmetry. Second, LsDia1 controls the intercellular chirality at the 3rd cleavage, which leads to the asymmetric *nodal* and *Pitx* expression at a specific cell at an early developmental stage. Third, we observe for the first time intracellular chirality at the fertilized one-cell stage dependent on LsDia1. The importance of actin-mediated cytoskeletal dynamics is increasingly recognized in the chiromorphogenesis of many animal phyla. Given that diaphanous orthologues are also present in human cells, studies on LsDia1 and LsDia2 may have implications for understanding situs inversus, a characteristic of 0.01% of the human population (Blum

Development (2019) 146, dev175976. doi:10.1242/dev.175976

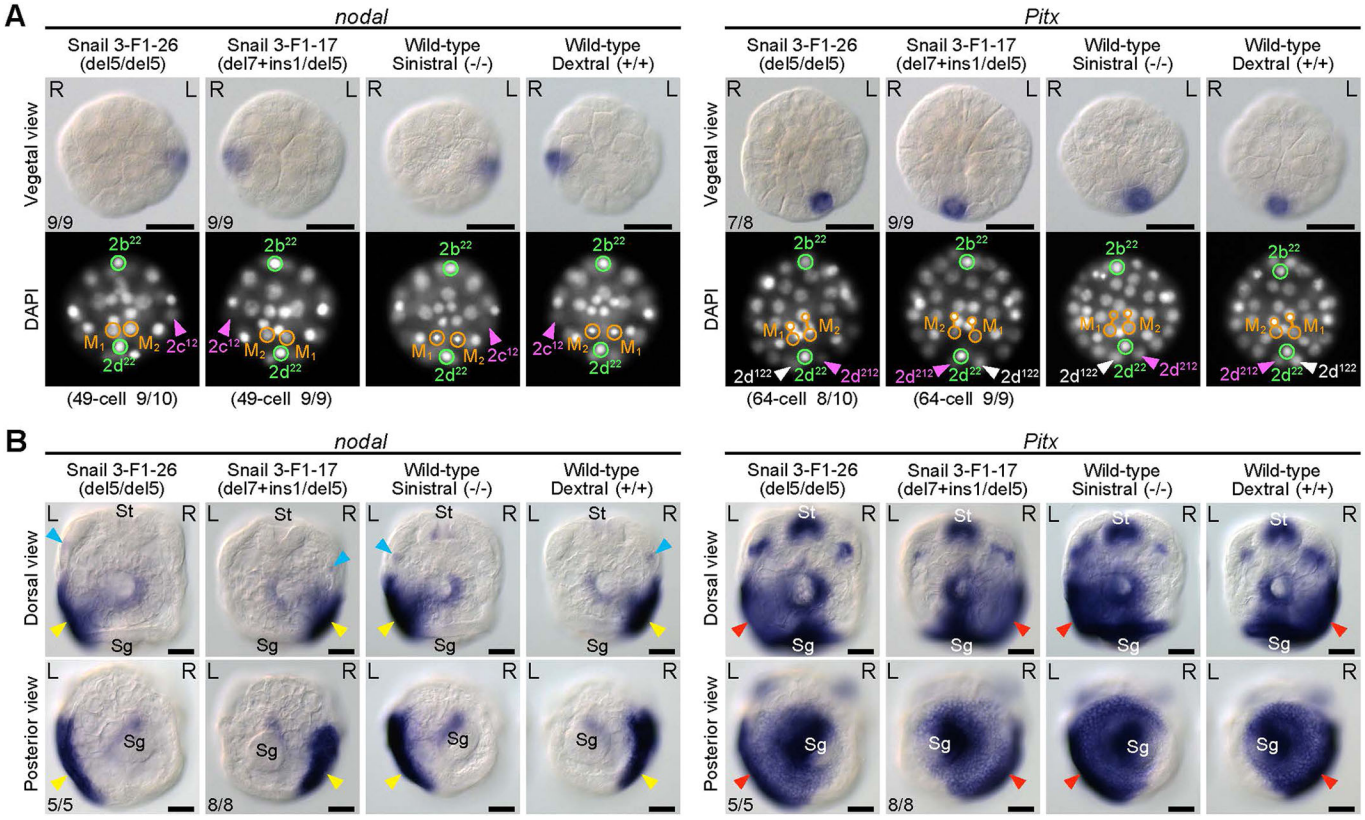

Fig. 4. *nodal* and *Pitx* expression patterns are mirror images according to the CRISPR/Cas9-mediated genotype. (A) Whole-mount *in situ* hybridization at the 49-cell stage for *nodal* and at the 64-cell stage for *Pitx* for the gene-edited F1 snails. Vegetal view (top) and DAPI (4′, 6-diamidino-2-phenylindole) staining to confirm the orientation and the developmental stage of the embryos (bottom). The midline goes between M_1 and M_2 cells, and connects $2b^{22}$ and $2d^{22}$ cells. Scale bars: 50 µm. (B) *nodal* and *Pitx* expression patterns at the late trochophore stage. Dorsal view (top) and posterior view (bottom). The sites of asymmetric expression are indicated by the blue arrowhead (cephalic ectoderm), the yellow arrowhead (lateral ectoderm near the shell gland) and the red arrowhead (posterolateral ectoderm). The *nodal* signal in the cephalic region was first detected in this work by improving the previous method (Kuroda et al., 2009). St, stomodeum; Sg, shell gland. Scale bars: 50 µm.

et al., 2014; Coutelis et al., 2014). Therefore, our work featuring formin-controlled early onset of chirality in *L. stagnalis* may provide new insight on unifying mechanisms in eukaryotes.

MATERIALS AND METHODS

Snails

Both the sinistral (−/−) and the dextral (+/+) wild-type strains of *L. stagnalis* used in this study have been maintained for many years from the original strain kindly supplied by G. Smit (Vrijie Universiteit, Amsterdam, The Netherlands). Genome-edited snails were created from this dextral strain. They were maintained under a 16/8 h light/dark cycle at 20-22°C and given fresh lettuce leaves and artificial food for tropical fish. All snail genome-editing experiments in this study were approved by the Tokyo University of Science (approval no. 1750/1751, 1873/1874), Japan. The care and use of animals were in accordance with the guidelines for animal experiments of Tokyo University of Science.

gRNA and Cas9 mRNA synthesis

To create the *Lsdia1*-targeting gRNA, a template plasmid vector was constructed by cloning the synthesized oligonucleotides for the target sequence (Fig. S1A) into BsmBI-digested pT7-gRNA vector (Addgene plasmid #46759) (Jao et al., 2013). The gRNA was generated by *in vitro* transcription from the BamHI-digested template plasmid using the MEGAscript T7 Kit (Ambion) and purified using the mirVana miRNA isolation kit (Ambion). The Cas9 nuclease mRNA was transcribed from NotI-digested pCS2-nCas9n vector (Addgene Plasmid #47929) (Jao et al., 2013) using the mMESSAGE mMACHINE SP6 kit (Ambion) and purified by phenol extraction and ethanol precipitation. The sequence comparison of *Lsdia1* and *Lsdia2* was performed using the ClustalX 1.83 program (Thompson et al., 1997).

Creating genome-edited snails by CRISPR/Cas9

A solution containing 100 ng/µl gRNA and 1500 ng/µl Cas9 mRNA diluted in nuclease-free water was injected into the dextral strain eggs at the one-cell stage according to our previously described protocol (Abe et al., 2009). Injected embryos and non-injected control embryos were cultured overnight in 5×HF solution (30 mM NaCl, 0.335 mM KCl, 0.34 mM $CaCl_2$, 0.1 mM $MgSO_4$, 0.12 mM $NaHCO_3$) based on Holtfreter's solution (Holtfreter, 1931). Some of these embryos were transferred to *ex ovo* culture in capillaries, as previously described (Kuroda et al., 2009), and were raised to adult snails (F0) individually. They produced the F1 generation by self-fertilization. The rest of the embryos were used for checking the genome-editing efficiency in the respective experiments by HMA (Fig. S1C). It has been reported that CRISPR/Cas9 can function in the early embryos of molluscs (Perry and Henry, 2015).

Heteroduplex mobility assay

The heteroduplex mobility assay (HMA) was used to analyse genome editing efficiency, and screening for germline transmission (Zhu et al., 2014; Ota et al., 2013, 2014). A 226 bp fragment including the target site was amplified from the *Lsdia1* sequence by using primers D1-MA4 detection Fw and D1-MA4 detection Rv (Fig. S1A). Each genomic DNA of adult snails was extracted from foot clips employing the Maxwell 16 Tissue DNA Purification Kit (Promega) and used as a PCR template. In the efficiency check for each injection experiment or screening for germline transmission, a small embryo was added directly to the PCR solution, and direct PCR amplification was performed by using KOD Fx Neo (Toyobo).

Development (2019) 146, dev175976. doi:10.1242/dev.175976

The PCR conditions for HMA were as follows: 96°C for 10 min; 35 cycles of 98°C for 10 s and 66°C for 30 s; followed by denaturation at 96°C for 3 min; and slow cooling to 20°C over 30 min. For the screening of germline transmission, the PCR products were run on 2% agarose gels and also sometimes on 10% polyacrylamide gels.

Phenotyping of shell coiling

All egg masses laid by genome-edited F0 snails and at least two egg masses by each genome-edited F1 and F2 snail were cultivated individually in a plastic petri dish at room temperature (20-22°C) until hatching. The control strains, dextral (+/+) and sinistral (−/−) were also studied similarly. The number of offspring in each egg mass was counted for the left- or the right-shell coiling. Although malformations were observed frequently in either shells or soft body, or both, they were not distinguished in this study. Those and juveniles with a swollen hydropic body were classified as abnormal embryos. The detailed analysis is summarized in the Figs S3A, S5A and Tables S1, S2. Photographs of the juveniles were taken using an Olympus SZX12 stereomicroscope equipped with an Olympus DP-70 CCD camera.

Genotyping

F1 snails were separated individually before sexual maturation, and genomic DNA was extracted from the foot clips. HMA was then performed on each snail as above. The PCR products were treated with Exo-SAP-IT (USB) and reacted directly with BigDye terminator v3.1 (Applied Biosystems) using D1-MA4 seq Rv primer (Fig. S1A). Genome-editing patterns for these products were analysed by using an ABI3130xl Genetic Analyzer (Applied Biosystems). The same genotyping analysis was performed on the following generations.

Third-cleavage pattern analysis

A fresh egg mass was collected from the individual genome-edited snail, dextral (+/+) or sinistral (−/−), and the one-cell-stage embryos were isolated from the capsule in 5×HF solution. Healthy looking four-cell embryos, near the third division time, were transferred to 5×HF solution in a small enclosure made of plastic tape on a glass slide and sealed with a cover slip. Time-lapse images of the third cleaving embryos were acquired on a Zeiss Axioskop 2 mot microscope equipped with a Zeiss 10× Plan-Neofluar objective lens and a Zeiss Axiocam MRc CCD camera, controlled by Zeiss Axiovision software. The data were obtained every 20 s or 30 s. The third cleavage pattern of each embryo was analysed visually, and the analysed data are summarized in Fig. 2A.

Protein detection

LsDia1 and β-tubulin protein detection by western blotting was performed as previously described (Kuroda et al., 2016). Fifty one-cell-stage embryos were obtained from one snail for each genotype and used as an SDS-PAGE sample for one lane. The following antibodies were used to probe the respective proteins: anti-LsDia1 (Kuroda et al., 2016; 1/10,000) and horseradish peroxidase (HRP)-conjugated anti-rabbit IgG (GE Healthcare, NA934; 1/50,000), anti-β-Tubulin (Sigma, TUB2.1; 1/20,000) and HRP-conjugated anti-mouse IgG (GE Healthcare, NA931; 1/50,000). The chemiluminescence signals were imaged using a ChemiDoc MP Imaging System (Bio-Rad) or a Luminescent Image Analyzer LAS-1000plus (FUJIFILM), and the images were analysed using Image Lab Software (Bio-Rad) or Image Gauge (FUJIFILM).

Whole-mount *in situ* hybridization

Whole-mount *in situ* hybridization for the *nodal* and *Pitx* genes was performed according to our standard protocols described previously (Kuroda et al., 2009, 2016). Digoxigenin-labelled antisense RNA probes were generated for their full-length coding sequences. Timing of fixing of embryos at the 49- or 64-cell stage was judged by observing the DAPI staining of embryos, whereas that for late trochophore-stage embryos was judged from their appearance. Stained embryo images were acquired using a Zeiss Axio Imager M1 microscope equipped with a Zeiss Axiocam MRc CCD camera.

Fluorescent staining

Four-cell or four- to eight-cell-stage embryos in the genome-edited snails, dextral (+/+) or sinistral (−/−) snails, were fixed in 4% paraformaldehyde in MTSTr [MTS buffer (pH 6.9), 0.1% Triton X-100] at 4°C overnight. Cytoskeleton staining was performed as described previously (Shibazaki et al., 2004; Kuroda et al., 2009, 2016). Confocal images were obtained using a Zeiss LSM 5 pascal laser scanning microscope equipped with a 20× Plan-Neofluar objective lens. The *z*-stack images were made from optical slices acquired every 10 µm along the animal-vegetal axis by using Zeiss LSM5 pascal software.

One-cell-stage chirality analysis

Trypsin treatment for removing the vitelline membrane of the fertilized eggs was performed as described by Meshcheryakov and Beloussov (1975). Crystalline trypsin (Wako) was dissolved in 5×HF before use to prepare a fresh solution at a concentration of 10 mg/ml. Embryos used were obtained from the population of dextral (+/+) or sinistral (−/−) and the individual genome-edited snails, 3-F4 (wt/del5) or (del5/del5), which were derived from one self-fertilized heterozygous snail, 3-F1-5-F2-1-F3-1 (wt/del5). The one-cell-stage embryos were isolated from the capsule and washed to remove adherent albumin in 5×HF. The embryos were transferred to the trypsin solution and incubated for 30 min at room temperature (21-23°C). Then the trypsinized embryos were carefully washed four times with fresh 5×HF and cultured until the first cleavage. Although the trypsinized embryos became fragile, the first cleavage initiated normally. Immediately after completion of the 1st cleavage, the trypsinized embryos were fixed in 4% paraformaldehyde in MTSTw [MTS buffer (pH 6.9), 0.1% Tween-20] for 30-120 min at room temperature and the chirality of each embryo was carefully observed. Depending on the degree and the rotational direction of the front blastomeres with respect to the rear ones when looking down from a direction perpendicular to the cleavage plane, they were classified as CW, weak CW, neutral, weak ACW and ACW.

Time-lapse imaging of the 1st cleavage

Time-lapse images of the 1st cleavage of the trypsinized embryos were acquired using an Olympus SZX12 stereomicroscope equipped with an Olympus DP-70 CCD camera, controlled by Olympus DP Controller software. The data were obtained every 20 s.

Statistical analysis

Statistical calculations were performed using Pearson's χ^2 test comparing the homozygous mutants against the wild-type dextral strain for number of sinistral juveniles, 3rd cleavage pattern and one-cell-stage chirality.

Acknowledgements

We thank Mr. S. Watanabe and Mr. K. Takanashi, and Mr. F. Ichikawa and Mr. H. Takahashi (graduate school students of Tokyo University of Science) for their help in collecting embryos and for their assistance in rearing gene-edited snails, respectively.

Competing interests

The authors declare no competing or financial interests.

Author contributions

Conceptualization: R.K.; Methodology: M.A., R.K.; Validation: R.K.; Formal analysis: M.A., R.K.; Investigation: M.A., R.K.; Resources: R.K.; Data curation: M.A., R.K.; Writing - original draft: R.K.; Writing - review & editing: R.K.; Supervision: R.K.; Project administration: R.K.; Funding acquisition: R.K.

Funding

This work was partly supported by the Japan Society for the Promotion of Science for Grants-in-Aid for Scientific Research, Challenging Exploratory Research (24657249 to R.K.).

Supplementary information

Supplementary information available online at http://dev.biologists.org/lookup/doi/10.1242/dev.175976.supplemental

References

Abe, M., Shimizu, M. and Kuroda, R. (2009). Expression of exogenous fluorescent proteins in early freshwater pond snail embryos. *Dev. Genes Evol.* **219**, 167-173. doi:10.1007/s00427-009-0278-8

Abe, M., Takahashi, H. and Kuroda, R. (2014). Spiral cleavages determine the left-right body plan by regulating Nodal pathway in monomorphic gastropods. *Physa acuta*. *Int. J. Dev. Biol.* **58**, 513-520. doi:10.1387/ijdb.140087rk

Asami, T., Gittenberger, E. and Falkner, G. (2008). Whole-body enantiomorphy and maternal inheritance of chiral reversal in the pond snail *Lymnaea stagnalis*. *J. Hered.* **99**, 552-557. doi:10.1093/jhered/esn032

Blum, M., Feistel, K., Thumberger, T. and Schweickert, A. (2014). The evolution and conservation of left-right patterning mechanisms. *Development* **141**, 1603-1613. doi:10.1242/dev.100560

Boycott, A. E. and Diver, C. (1923). On the inheritance of sinistrality in *Lymnaea peregra*. *Proc. R. Soc. Biol. Sci. Ser. B* **95**, 207-213. doi:10.1098/rspb.1923.0033

Coutelis, J.-B., González-Morales, N., Géminard, C. and Noselli, S. (2014). Diversity and convergence in the mechanisms establishing L/R asymmetry in metazoa. *EMBO Rep.* **15**, 926-937. doi:10.15252/embr.201438972

Danilchik, M. V., Brow, E. E. and Riegert, K. (2006). Intrinsic chiral properties of the Xenopus egg cortex: an early indicator of left-right asymmetry? *Development* **133**, 4517-4526. doi:10.1242/dev.02642

Davison, A., McDowell, G. S., Holden, J. M., Johnson, H. F., Koutsovoulos, G. D., Liu, M. M., Hulpiau, P., Van Roy, F., Wade, C. M., Banerjee, R. et al. (2016). Formin is associated with left-right asymmetry in the pond snail and the frog. *Curr. Biol.* **26**, 654-660. doi:10.1016/j.cub.2015.12.071

Freeman, G. and Lundelius, J. W. (1982). The developmental genetics of dextrality and sinistrality in the gastropod *Lymnaea peregra*. *Wilehm Rouxs Arch. Dev. Biol.* **191**, 69-83. doi:10.1007/BF00848443

González-Morales, N., Géminard, C., Lebreton, G., Cerezo, D., Coutelis, J. B. and Noselli, S. (2015). The atypical cadherin dachsous controls left-right asymmetry in *Drosophila*. *Dev. Cell* **33**, 675-689. doi:10.1016/j.devcel.2015.04.026

Grande, C. and Patel, N. H. (2009). Nodal signalling is involved in left-right asymmetry in snails. *Nature* **457**, 1007-1011. doi:10.1038/nature07603

Holtfreter, J. (1931). Über die aufzucht isolierter teile des amphibienkeimes: II. Züchtung von keimen und keimteilen in salzlösung. *Wilhelm Roux Arch. Entwickl. Mech. Org.* **124**, 404-466. doi:10.1007/BF00652482

Hoso, M., Kameda, Y., Wu, S.-P., Asami, T., Kato, M. and Hori, M. (2010). A speciation gene for left-right reversal in snails results in anti-predator adaptation. *Nat. Commun.* **1**, 133. doi:10.1038/ncomms1133

Hosoiri, Y., Harada, Y. and Kuroda, R. (2003). Construction of a backcross progeny collection of dextral and sinistral individuals of a freshwater gastropod, *Lymnaea stagnalis*. *Dev. Genes Evol.* **213**, 193-198. doi:10.1007/s00427-003-0315-y

Jao, L.-E., Wente, S. R. and Chen, W. (2013). Efficient multiplex biallelic zebrafish genome editing using a CRISPR nuclease system. *Proc. Natl. Acad. Sci. USA* **110**, 13904-13909. doi:10.1073/pnas.1308335110

Jinek, M., Chylinski, K., Fonfara, I., Hauer, M., Doudna, J. A. and Charpentier, E. (2012). A programmable dual-RNA-guided DNA endonuclease in adaptive bacterial immunity. *Science* **337**, 816-821. doi:10.1126/science.1225829

Juan, T., Géminard, C., Coutelis, J.-B., Cerezo, D., Polès, S., Noselli, S. and Fürthauer, M. (2018). Myosin1D is an evolutionarily conserved regulator of animal left–right asymmetry. *Nat. Commun.* **9**, 1942. doi:10.1038/s41467-018-04284-8

Kuroda, R. (2014). How a single gene twists a snail. *Integr. Comp. Biol.* **54**, 677-687. doi:10.1093/icb/icu096

Kuroda, R. (2015). A twisting story: how a single gene twists a snail? Mechanogenetics. *Q. Rev. Biophys.* **48**, 445-452. doi:10.1017/S0033583515000098

Kuroda, R., Endo, B., Abe, M. and Shimizu, M. (2009). Chiral blastomere arrangement dictates zygotic left-right asymmetry pathway in snails. *Nature* **462**, 790-794. doi:10.1038/nature08597

Kuroda, R., Fujikura, K., Abe, M., Hosoiri, Y., Asakawa, S., Shimizu, M., Umeda, S., Ichikawa, F. and Takahashi, H. (2016). Diaphanous gene mutation affects spiral cleavage and chirality in snails. *Sci. Rep.* **6**, 34809. doi:10.1038/srep34809

Martindale, M. Q. (1986). The 'organizing' role of the D quadrant in an equal cleaving spiralian, *Lymnaea stagnalis* as studied by UV laser deletion of macromeres at intervals between third and fourth quartet formation. *Int. J. Invert. Reprod. Dev.* **9**, 229-242. doi:10.1080/01688170.1986.10510198

Meshcheryakov, V. N. and Beloussov, L. V. (1975). Asymmetrical rotations of blastomeres in early cleavage of gastropoda. *Wilehm Roux Arch. Dev. Biol.* **177**, 193-203. doi:10.1007/BF00848080

Morrill, J. B. (1998). Cellular patterns and morphogenesis in early development of freshwater pulmonate snails, *Lymnaea* and *Physa* (Gastropoda, Mollusca). In *Reproductive Biology of Invertebrates, Volume 7, Progress in Developmental Biology* (ed. K.G. Adiyodi and R.G. Adiyodi), pp. 67-107. New York: Wiley, Inc.

Nakamura, T. and Hamada, H. (2012). Left-right patterning: conserved and divergent mechanisms. *Development* **139**, 3257-3262. doi:10.1242/dev.061606

Ota, S., Hisano, Y., Muraki, M., Hoshijima, K., Dahlem, T. J., Grunwald, D. J., Okada, Y. and Kawahara, A. (2013). Efficient identification of TALEN-mediated genome modifications using heteroduplex mobility assays. *Genes Cells* **18**, 450-458. doi:10.1111/gtc.12050

Ota, S., Hisano, Y., Ikawa, Y. and Kawahara, A. (2014). A. Multiple genome modifications by the CRISPR/Cas9 system in zebrafish. *Genes Cells* **19**, 555-564. doi:10.1111/gtc.12154

Perry, K. J. and Henry, J. Q. (2015). CRISPR/Cas9-mediated genome modification in the mollusc, *Crepidula fornicata*. *Genesis* **53**, 237-244. doi:10.1002/dvg.22843

Schonegg, S., Hyman, A. A. and Wood, W. B. (2014). Timing and mechanism of the initial cue establishing handed left–right asymmetry in *Caenorhabditis elegans* embryos. *Genesis* **52**, 572-580. doi:10.1002/dvg.22749

Shibazaki, Y., Shimizu, M. and Kuroda, R. (2004). Body handedness is directed by genetically determined cytoskeletal dynamics in the early embryo. *Curr. Biol.* **14**, 1462-1467. doi:10.1016/j.cub.2004.08.018

Sturtevant, A. H. (1923). Inheritance of direction of coiling in *Lymnaea*. *Science* **58**, 269-270. doi:10.1126/science.58.1501.269

Taniguchi, K., Maeda, R., Ando, T., Okumura, T., Nakazawa, N., Hatori, R., Nakamura, M., Hozumi, S., Fujiwara, H. and Matsuno, K. (2011). Chirality in planar cell shape contributes to left-right asymmetric epithelial morphogenesis. *Science* **333**, 339-341. doi:10.1126/science.1200940

Tee, Y. H., Shemesh, T., Thiagarajan, V., Hariadi, R. F., Anderson, K. L., Page, C., Volkmann, N., Hanein, D., Sivaramakrishnan, S., Kozlov, M. M. et al. (2016). Cellular chirality arising from the self-organization of the actin cytoskeleton. *Nat. Cell Biol.* **17**, 445-457. doi:10.1038/ncb3137

Thompson, J. D., Gibson, T. J., Plewniak, F., Jeanmougin, F. and Higgins, D. G. (1997). The CLUSTAL_X Windows interface: Flexible strategies for multiple sequence alignment aided by quality analysis tools. *Nucleic Acids Res.* **25**, 4876-4882. doi:10.1093/nar/25.24.4876

Tingler, M., Kurz, S., Maerker, M., Ott, T., Fuhl, F., Schweickert, A., LeBlanc-Straceski, J. M., Noselli, S. and Blum, M. (2018). A conserved role of the unconventional myosin 1d in laterality determination. *Curr. Biol.* **28**, 810-816. doi:10.1016/j.cub.2018.01.075

Vandenberg, L. N. and Levin, M. (2013). A unified model for left-right asymmetry? Comparison and synthesis of molecular models of embryonic laterality. *Dev. Biol.* **379**, 1-15. doi:10.1016/j.ydbio.2013.03.021

Wan, L. Q., Ronaldson, K., Park, M., Taylor, G., Zhang, Y., Gimble, J. M. and Vunjak-Novakovic, G. (2011). Micropatterned mammalian cells exhibit phenotype-specific left-right asymmetry. *Proc. Natl. Acad. Sci. USA* **108**, 12295-12300. doi:10.1073/pnas.1103834108

Zhu, X., Xu, Y., Yu, S., Lu, L., Ding, M., Cheng, J., Song, G., Gao, X., Yao, L., Fan, D. et al. (2014). An efficient genotyping method for genome-modified animals and human cells generated with CRISPR/Cas9 system. *Sci. Rep.* **4**, 6420. doi:10.1038/srep06420